

MECHANISM OF OPTICAL VORTEX GENERATION FROM SELF-ASSEMBLED TFCD ARRAY IN SMECTIC LC AND TFCD APPLICATION TO OPTICAL DEVICES

K. KÄLÄNTÄR

Japan Global Optical Solutions, R&D Center, 2-50-9 Sanda-Cho, Hachi-Ouji-Shi, Tokyo 193-0832, Japan

The smectic liquid crystal (SmLC) is used to fabricate an array of self-assembled defects in which each has a spindle torus structure. Each defect is a toroidal focal conic domain (TFCD) with an optical vortex generation function. The mechanism of optical vortex generation in TFCD was studied in details and found that a TFCD is an integration of radial graded-index (GRIN) layers and axially GRIN shells. The light focusing and polarization transformation characteristics of the GRIN layers are formulated to realize a single millimetric optical device with vortex generation function.

Keywords: Optical vortex, Focal Conic Defect, Toroidal FCD, Smectic LC, Graded Index, GRIN

PACS: 64.70; 61.46; 61.30

1. INTRODUCTION

Optical vortex or phase singularity generation has been found to be one of the challengeable topics in the integrated optics [1]. The space-variant polarization, (transversely nonuniform), and dislocations such as optical vortices (Fig.1) are studied and applied to high resolution microscopy development, optical manipulation, quantum computing, and astronomical imaging. Single optical vortex generating devices have been reported in recent years. However, the requirements for an array of optical vortices in large size have also been increasing for applications such as opto-mechanical pumping, multichannel optical communicating, quantum computing, and astronomical holography.

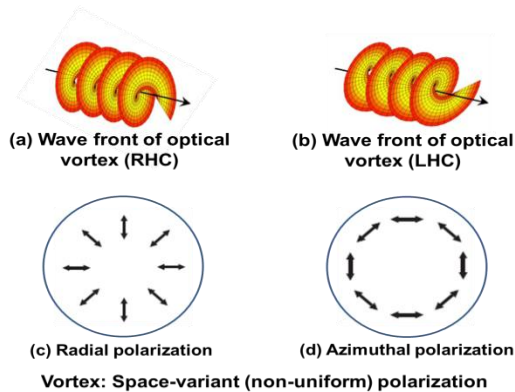


Fig. 1. Helical wave fronts or optical vortices and radial / azimuthal polarizations

Optical beam with helical wave front, i.e., an optical vortex; (a) right hand circular (RHC) wave front, (b) left hand circular (LHC) wave front. Space-variant polarizations; (c) radial polarization. (d) azimuthal polarization.

Variety of methods have been developed to generate optical vortex arrays, such as electron-beam, lithography, photo-polymerization, and direct laser writing of radial birefringence. Among these methods liquid crystals (LCs) have been used to generate optical vortex arrays because of quick and simple stabilization of molecular ordering and structure. Recent studies show the realization of arrays of microscopic optical vortex generators using cholesteric or nematic LCs [2].

However the mechanism of optical generation in toroidal focal conic defect (TFCD) has not been reported yet. In this study, the vortex array generation was analyzed and the light field propagation was clarified in a single smectic LC (SmLC) TFCD [3]-[4]. The analysis results are reflected on fabrication of a novel millimeter order single optical vortex generator, namely a novel optical device.

2. STRUCTURING TFCD ARRAY

Among the aforementioned methods SmLC is used for TFCD fabrication because of quick and simple stabilization of molecular ordering and structure. To fabricate TFCDs, the crystalline LC material is deposited on the substrate, and the substrate is heated to temperature exceeding 65 °C, i.e., corresponding to the isotropic phase of the LC. The glass substrate is cooled at a rate of -5°C/min to form the smectic A phase. The TFCDs are self-assembled on the substrate.

In this study the vortex array generation was analyzed in a single torus SmLC defect to clarify the behavior of light field propagation in the TFCD.

3. TFCD STRUCTURE

In the aforementioned fabrication method the SmLC defects are self-assembled in a large number (about 1000 TFCDs). Each defect is a TFCD that generates optical vortex. The fabricated feature size is about 35 μm.

The geometry of a TFCD is shown in a cylindrical coordinate systems in Fig.2. A TFCD is found to be a spindle torus as shown the cross section in Fig.3. The TFCD cross-section is defined as B₁C₁C₂AB₂ in Fig.3. The status of SmLC directors are shown at point B₁ and C₁ in gray colors. The bottom director is in ρ-direction (or y-axis) in cylindrical coordinate system. These directors are distributed along ρ-axis, i.e., from side walls (B₁B₂ or C₁C₂) toward the center of the TFCD. The extraordinary refractive index (director laid on the bottom of the TFCD along ρ) is n_e [n_e(ρ,π/2)] for propagated light wave along the z-axis (θ=π/2). The directors are standing up gradually with decrease in zenith angle, and finally are vertical along the B₁B₂ or C₁C₂. The refractive index (director standing up along the wall of the TFCD) is n_o [n_o(ρ_{max}/2,0)] for the propagating light along the z-axis. The refractive index difference along the vertical axis of

TFCD (z-axis) at an arbitrary ρ is given by the following equation,

$$\Delta n(\rho, \theta) = \frac{n_o\left(\frac{\rho_{max}}{2}, 0\right) \times n_e\left(\rho, \frac{\pi}{2}\right)}{\sqrt{n_e^2\left(\rho, \frac{\pi}{2}\right) \times \cos^2 \theta + n_o^2\left(\frac{\rho_{max}}{2}, 0\right) \times \sin^2 \theta}} - n_o\left(\frac{\rho_{max}}{2}, 0\right) \quad (1)$$

The first term is the effective local refractive index of the extraordinary wave. The zenith angle θ is given by

$$\theta = \frac{\pi}{2} - \tan^{-1}\left(\frac{z}{\frac{\rho_{max}}{2} - \rho}\right) \quad (2)$$

Since the directors are perpendicular to the radius of the spindle torus, i.e., the front surface of the TFCD, there is small differences between the TFCD height at the center ($\rho=0$) and that at the side wall boundaries. Because a TFCD is a part of torus, the aspect ratio is 1:1, i.e., the diameter of the TFCD is equal to its height (Fig.3). The height of TFCD (on the front surface, z_s) at an arbitrary ρ is given

$$z_s(\rho) = \sqrt{\rho_{max}^2 - \left(\frac{\rho_{max}}{2} - \rho\right)^2} \quad (3)$$

Using the above equations, the normalized refractive index difference can be shown by the following equation.

$$\frac{\Delta n(\rho, \theta)}{\Delta n_{max}} \approx \sin^2(\rho, \theta) \quad (4)$$

The TFCD has a funnel shape front surface. The height variation, i.e., Eq.(3) is shown in Fig.4.

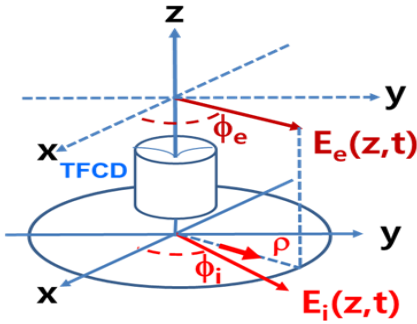


Fig.2 Geometry of a TFCD

Cylindrical coordinate system is used to show the polarization transformation of the TFCD. $E_e(z,t)$ at azimuth angle of ϕ_e is the amplitude of the incident electric field and $E_i(z,t)$ at ϕ_i is the emergent electric field.

The normalized refractive index difference causes phase change of the propagating light. The normalized refractive index has a $\sin^2(\rho, \theta)$ variation. Therefore, the squared sine is used for the normalized refractive index variation and for calculating the phase change.

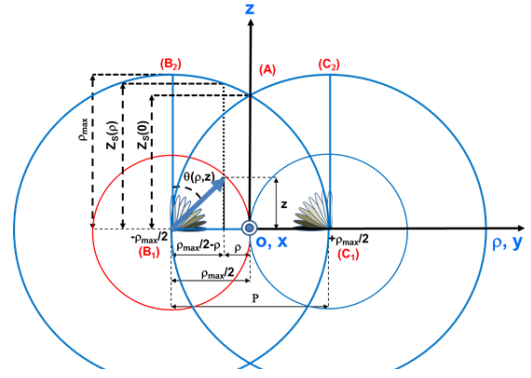


Fig.3. TFCD structure

Outer overlapped circles are the cross section of a spindle torus. The rectangle of $B_1C_1C_2B_2$ is the cross section of the TFCD.

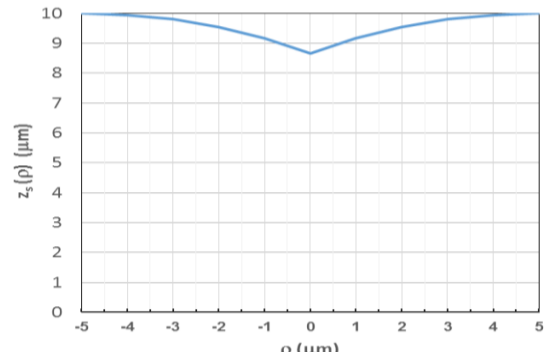


Fig.4. TFCD's height vs. radius

Front surface of TFCD has a shape of funnel. The cross section of the funnel is plotted versus the radius of the TFCD (cylindrical body).

The normalized phase is plotted versus ρ and z as in Fig.5.

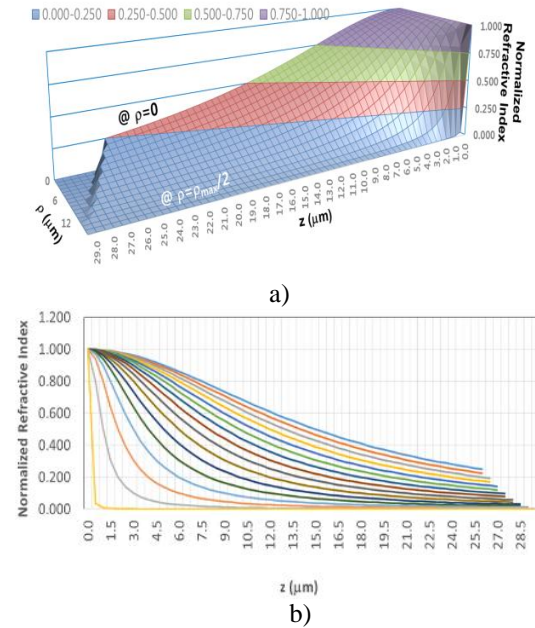


Fig.5. Parabolic refractive index distribution

On axis refractive index changes from n_e to n_o .

(a) Normalized refractive index along ρ and z in the TFCD.

(b) Normalized refractive index along z-axis.

The refractive index on the bottom of the TFCD is n_e that is decreasing along the z -axis.

4. PHASE RETARDATION

The phase retardation is calculated in terms of wavelength, thickness and birefringence distribution of optical media. Because the direction of molecular director varies along the propagation axis (z -axis), the birefringence should be integrated over the propagation path to get averaged effective birefringence. The resultant averaged phase retardation at an arbitrary position (ρ_0) is given by the following equation

$$\Delta\Phi(\rho_0, z_s) = \frac{2\pi\Delta n_{\max}}{\lambda} \int_0^{z_s} \sin^2 \left[\frac{\pi}{2} - \tan^{-1} \left(\frac{z}{\frac{\rho_{\max}}{2} - \rho_0} \right) \right] dz \tag{5}$$

Eq.(5) shows the variation of the phase along the z -axis as well as the ρ -axis. This is due to refractive index change along the z -axis and ρ -axis that is shown schematically in Fig.6.

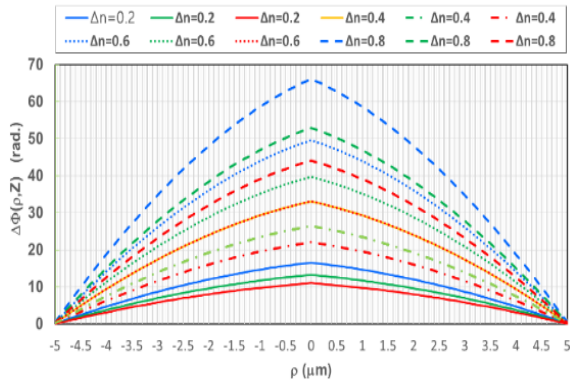


Fig.6. Phase retardation along the z -axis
Refractive index variation along z -axis at arbitrary radius results in phase retardation [$\approx \sin^2(\rho, \theta)$] along the z -axis that changes with wavelength. The blue, green and red colors represents the wavelengths of 400, 500 and 600 nm. Two graphs have been overlapped.

The circular polarized light transmitted through TFCD has a phase difference with respect to original incident beam and has an intensity given in Eq.(6) as below. Here K is the fraction of the original light ($K \leq 1$). Final polarization distribution of output field modulated by TFCD is characterized by Jones matrix of the optical system:

$$\left| \mathbf{E}_{\text{out}}(\rho, \phi, z) \right|^2 = \left[\cos(m\phi) * \sin \left[\frac{\Delta\Phi(\rho, z)}{2} \right] \right]^2 + \left[\sin(m\phi) * \sin \left[\frac{\Delta\Phi(\rho, z)}{2} \right] \right]^2 + \cos \left[\frac{\Delta\Phi(\rho, z)}{2} \right] K \tag{6}$$

Here, m is a topological charge that designates the number of cyclic changes in polarization state or phase along a closed path surrounding the center of the beam, defined as $m=2q$. This parameter is an integer value when the medium is rotationally symmetric. The topological charge (m) is twice the topological strength (q).

Substituting these parameters into the Jones matrix, the TFCD's Jones matrix can be obtained. Using the Eq.(6), the coronagraphs of the transmitted light wave and vortices can be obtained on the TFCDs. The term of squared *cosine* changes with azimuth angle, resulting bright and dark zones. The term of squared *sine* changes with phase retardation in which the retardation itself changes with ρ and z or θ . The multiplication of these two functions results in a coronagraph (not shown) in which the zero-intensity regions; the dark rings and dark Maltese cross along the radial and azimuthal directions. The bright and dark regions are the spatially polarization changing areas, presenting vortices.

5. TFCD AS GRIN LAYERS AND GRIN SHELLS

As explained the refractive index of a TFCD in Eq.(4), a TFCD can be assumed as an integration of graded-index (GRIN) layers (in ρ -direction) (Fig.7(a)) that have parabolic refractive index distributions with different on-axis refractive indices and focusing parametric. The refractive index distribution of a TFCD is shown in Fig.7(b).

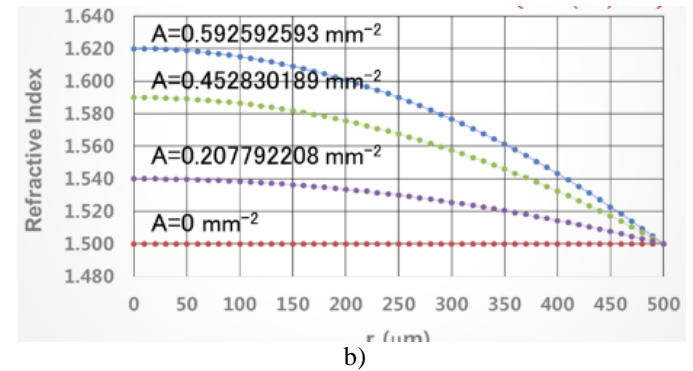
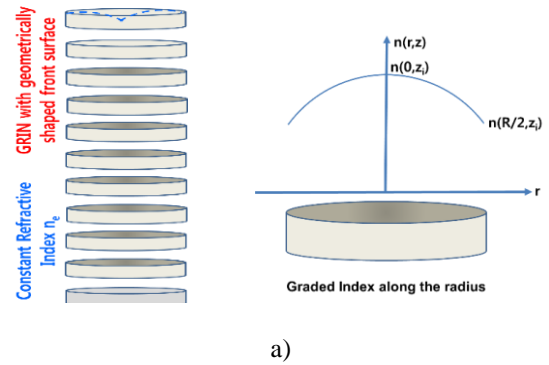


Fig.7. Parabolic refractive index distribution (Eq.7)
a) On axis refractive index changes from n_e to n_0 . The bottom and side wall refractive indices, n_e and n_0 , are constant ($r \cong \rho$). Focusing parameter (A) is different for each layer.

In addition the refractive index change can be extended to vertical direction and assumed that a TFCD is an integration of GRIN shells as shown schematically the structure in Fig.8 (a) and (b).

Each layer (disc shape) has a parabolic refractive index distribution that has a light focusing characteristic. The parabolic refractive index is given by the following equation in which the focusing parameter is given by "A".

$$n_G(\rho) = n_G(0) \left\{ 1 - \left(\sqrt{\frac{A}{2}} \right)^2 \rho^2 \right\} \quad (7)$$

Since two types of light rays exist in a medium with parabolic refractive index distribution, Eq.(7) is a common refractive index distribution for both meridional and helical rays.

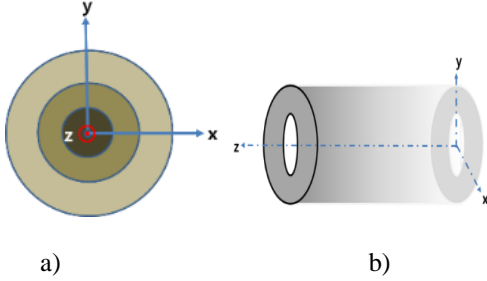


Fig.8 Parabolic refractive index distribution for each layer along z axis.

On axis refractive index changes from n_c to side wall refractive index, n_o . (a) Top view of the shells, (b) Perspective of a single shell.

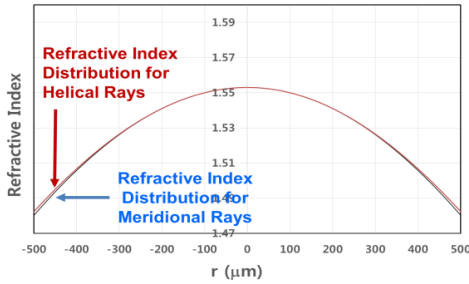


Fig.9. Parabolic refractive index distribution for each TFCD layer. The distributions for helical and meridional rays.

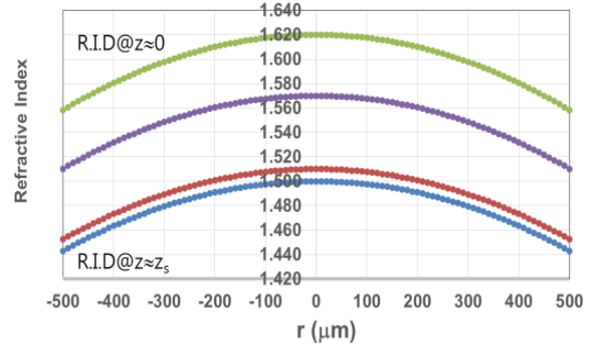


Fig.10. Parabolic refractive index distribution for each layer The center refractive index is different for each layer and changes with z as well as r ($r \equiv \rho$).

The difference in the optimized refractive index distributions are shown in Fig.9. The refractive index distributions for the layers are shown in Fig.10.

6. CONCLUSIONS

The mechanism of optical vortices generation from toroidal focal conic domains that are self-aligned in SmLC was studied to realize a functional optical device in millimetric size to generate a single or multi-phase singularities. The refractive index distribution and the phase retardation for a single TFCD were formalized. The Jones matrix of the TFCD for vortex generation and layer light transmission were developed. The structure of a single TFCD was found to be an integration of graded-index horizontal layers (in ρ -direction) or vertical shells (in z -direction). The analogue integration of thin GRIN layers can lead to realization of a single TFCD for optical vortex generation.

[1] B.S. Son, S.J. Kim, Y.H. Kim, K. Käläntär, H.M Kim, H.S. Jeong, S.Q. Choi, J.H. Shin, H.T. Jung, and Y.H. Lee: “Optical vortex arrays from smectic liquid Crystals,” Vol. 22, No. 4/OE.22.004699 (Feb.2014).
 [2] R. Barboza, U. Bortolozzo, G. Assanto, E. Vidal-Henriquez, M. G. Clerc, and S. Residori. “Harnessing optical vortex lattices in nematic liquid crystals,” Phys. Rev. Lett. 111(9), 093902 (2013).
 [3] D.K. Yoon, M.C. Choi, Y.H. Kim, M.W. Kim,

O.D. Lavrentovich, H.T. Jung. “Internal structure visualization and lithographic use of periodic toroidal holes in liquid crystals,” Nature Materials 6, 866 - 870 (October 2007).
 [4] Y.H. Kim, D.K. Yoon, H.S. Jeong, H.T. Jung. “Self-assembled periodic liquid crystal defects array for soft lithographic template,” Soft Matter 6 (7), 1426-1431, 2010.

Receivied: 29.03.2018